

Design of Bioactive Peptides from Naturally Occurring μ -Conotoxin Structures*^[5]

Received for publication, April 27, 2012, and in revised form, June 25, 2012. Published, JBC Papers in Press, July 6, 2012, DOI 10.1074/jbc.M112.375733

Marijke Stevens^{‡1}, Steve Peigneur[‡], Natalia Dyubankova[§], Eveline Lescrinier[§], Piet Herdewijn[§], and Jan Tytgat^{‡2}

From the [‡]Laboratory of Toxicology, Katholieke Universiteit (KU) Leuven, Campus Gasthuisberg O and N2, Herestraat 49 Box 922, 3000 Leuven, Belgium and [§]Laboratory of Medicinal Chemistry, Rega Institute for Medical Research, KU Leuven, Minderbroedersstraat 10, 3000 Leuven, Belgium

Background: μ -Conotoxins possess interesting blocking effects on voltage-gated sodium channels (Na_v s).

Results: Based on two known μ -conotoxins, we designed miniaturized peptides that potently and selectively block Na_v s, although they do not contain an α -helix.

Conclusion: Peptidomimetics constitute a valuable tool to develop novel, synthetic Na_v blockers.

Significance: Our compounds prove to be an ideal starting platform in the search for therapeutics to treat Na_v -related diseases.

To date, cone snail toxins (“conotoxins”) are of great interest in the pursuit of novel subtype-selective modulators of voltage-gated sodium channels (Na_v s). Na_v s participate in a wide range of electrophysiological processes. Consequently, their malfunctioning has been associated with numerous diseases. The development of subtype-selective modulators of Na_v s remains highly important in the treatment of such disorders. In current research, a series of novel, synthetic, and bioactive compounds were designed based on two naturally occurring μ -conotoxins that target Na_v s. The initial designed peptide contains solely 13 amino acids and was therefore named “Mini peptide.” It was derived from the μ -conotoxins KIIIA and BuIIIC. Based on this Mini peptide, 10 analogues were subsequently developed, comprising 12–16 amino acids with two disulfide bridges. Following appropriate folding and mass verification, blocking effects on Na_v s were investigated. The most promising compound established an IC_{50} of 34.1 ± 0.01 nM (R2-Midi on $\text{Na}_v1.2$). An NMR structure of one of our most promising compounds was determined. Surprisingly, this structure does not reveal an α -helix. We prove that it is possible to design small peptides based on known pharmacophores of μ -conotoxins without losing their potency and selectivity. These data can provide crucial material for further development of conotoxin-based therapeutics.

Voltage-gated sodium channels (Na_v s)³ are important transmembrane proteins with respect to generating as well as propagating action potentials in excitable cells (e.g. neuronal cells

and muscular cells). Defective Na_v s cause several diseases or channelopathies like epileptic disorders (1), neuromuscular diseases (2), and cardiomyopathies (3). Blocking the aberrant Na^+ current can be effective in treating these disorders. In the past, nonspecific Na_v blockers like antiepileptic drugs, anticonvulsants, or antiarrhythmics have been widely utilized as therapeutics (4). However, their use remains limited due to unwanted side effects. More selective Na_v s blockers are needed.

One group of peptides recently acquiring interest in this respect is conotoxins. Conotoxins are biologically active compounds isolated from the venom of cone snails (genus *Conus*). Four families of conotoxins target Na_v s. These are categorized according to either their functional agonistic or antagonistic effects. δ -Conotoxins (5) and ι -conotoxins (6) produce agonistic effects, whereas μO -conotoxins (7) and μ -conotoxins (8) bring about antagonistic effects. Several excellent reviews exist on their discovery, description, and therapeutic potential (9–11). The group of toxins that is of importance in the current study is the μ -conotoxin family.

μ -Conotoxins display a typical folding pattern called framework III. In this conformation, three conserved disulfide bridges are formed between Cys^1 - Cys^4 , Cys^2 - Cys^5 , and Cys^3 - Cys^6 (Cys residues are numbered according to their order in the total sequence) (9). They affect Na_v s by plugging into the pore analogously to the guanidinium toxins tetrodotoxin and saxitoxin. However, they do not target precisely the same binding area (12). Other contact points on the outer channel vestibule are possibly also essential with respect to their binding (12–17).

It is their high potency as well as small size (16–26 AAs) and selectivity that renders μ -conotoxins very interesting (18). The latter characteristic in particular is a valuable quality for the development of potential therapeutics. In our experiments, we attempted to benefit from this feature. Our strategy was to miniaturize μ -conotoxins as much as possible as well as to improve their potency and selectivity. In addition, the peptides needed to be druggable compounds, e.g. compounds that could be synthesized economically. Removal of one disulfide bridge for instance offers a large economic advantage. Moreover, it can provide extra stability because reactive thiol groups of disulfide bridges can catalyze degradation processes (19).

* This work was supported in part by Fonds Wetenschappelijk Onderzoek Vlaanderen Grants G.0257.08 and G.0433.12, KU Leuven Grant OT/12/081, and Interuniversity Attraction Poles Program, Belgian State, Belgian Science Policy Grant IUAP 7/12.

[5] This article contains supplemental Figs. S1 and S2.

The atomic coordinates and structure factors (code 2LU6) have been deposited in the Protein Data Bank, Research Collaboratory for Structural Bioinformatics, Rutgers University, New Brunswick, NJ (<http://www.rcsb.org/>).

¹ Holds a fellowship from the Belgian Wetenschappelijk Onderzoek Multiple Sclerose Foundation.

² To whom correspondence should be addressed. Tel.: 32-16-32-34-04; Fax: 32-16-32-34-05; E-mail: Jan.Tytgat@pharm.kuleuven.be.

³ The abbreviations used are: Na_v , voltage-gated sodium channel; AA, amino acid.

Our starting point was a small and stable peptide of 13 AAs derived from two naturally occurring μ -conotoxins, KIIIA from *Conus kinoshitai* (20), and BuIIIC from *Conus bullatus* (21). A series of 10 analogues were subsequently designed. Although they only comprise 13–16 amino acids, all peptides retained their blocking properties. Our most promising compound exhibits an IC_{50} value of 34.1 nM on $\text{Na}_v1.2$. In addition to being a very potent blocker, it displays an interesting selectivity for $\text{Na}_v1.2$ over $\text{Na}_v1.4$ and $\text{Na}_v1.6$. An NMR structure of one of our most promising compounds, named Midi, was determined. Surprisingly, this structure does not reveal an α -helix. This unique feature has never been seen in any of the known μ -conotoxins.

EXPERIMENTAL PROCEDURES

Chemical Synthesis of Synthetic Peptides and Analysis—The following peptides were synthesized by Peptide 2.0 (Chantilly, VA): Mini, Mini-R5A, Mini-R5E, Midi, Extra-Mini, EAD-Midi, EAK-Midi, AA-Midi, and a Midi peptide with the following requirements: a first disulfide bridge between Cys^1 - Cys^{13} and a second bridge between Cys^3 - Cys^{14} . The R-analogues of the Midi peptide (R1-Midi, R2-Midi, and R3-Midi) were synthesized by Shanghai Mocell Biotech (Shanghai, China). Purity was confirmed to be $\geq 95\%$ by reversed-phase HPLC on an analytical Vydac C_{18} column (218MS54, 4.6×250 mm, $5\text{-}\mu\text{m}$ particle size; Grace, Deerfield, IL) with a flow rate of $1\text{ ml}\cdot\text{min}^{-1}$. UV absorbance was monitored at 214 and 280 nm with a dual wavelength absorbance detector. A linear gradient of 0–40% acetonitrile in 40 min was used at a flow rate of $1\text{ ml}\cdot\text{min}^{-1}$. The gradient was set by means of a mixture of solvent A (0.085% (v/v) trifluoroacetic acid (TFA) in acetonitrile) and solvent B (0.1% TFA (v/v) in water) with an initial concentration of 0% solvent A. Molecular masses were validated on an LCQ Deca XP electrospray ionization-quadrupole ion trap-mass spectrometer (Thermo Finnigan) in a positive ionization mode.

Folding of the Peptides—The Mini peptide was folded using two strategies. The first strategy was executed in accordance with previous strategies established by our laboratory (22) and other groups (e.g. Ref. 23). A glutathione folding mixture was prepared that contained 1 mM reduced glutathione, 1 mM oxidized glutathione, 1 mM EDTA, and 100 mM Tris-HCl (pH 7.5). The reduced Mini peptide was dissolved in 0.01% (v/v) TFA before being added to the folding mixture with a final peptide concentration of 112 μM . At different time points (e.g. 30 s, 30 min, 24 h, and 1 week) subsequent to initiation of the folding reaction, aliquots were withdrawn and quenched by acidification with 8% formic acid. In the second folding strategy, peptides were dissolved in the physiological buffer solution ND-96 (see “Heterologous Expression”). Folding mixtures were retained at room temperature for at least 2–3 days. At different time points following dissolution, aliquots were withdrawn. Aliquots were analyzed with reversed-phase HPLC by means of an analytical Vydac C_{18} column as described in the previous section. Masses of the folded peptides were validated by electrospray ionization MS.

Heterologous Expression—Complementary DNA encoding the Na_v channels was subcloned into the corresponding vector: $\text{rNa}_v1.2/\text{pLCT1}$ (NotI), $\text{rNa}_v1.3/\text{pNa3T}$ (NotI), $\text{rNa}_v1.4/\text{pUI-2}$

(NotI), $\text{hNa}_v1.5/\text{pcDNA3.1}$ (XbaI), $\text{mNa}_v1.6/\text{pLCT1}$ (NotI), $\text{rNa}_v1.7/\text{pBSTA.rPN1}$ (SacII), $\text{rNa}_v1.8/\text{pSP64T}$ (XbaI), $\text{h}\beta 1/\text{pGEM-HE}$ (NheI), or $\text{r}\beta 1/\text{pSP64T}$ (EcoRI). Following linearization with the respective restriction enzymes (indicated in parentheses), capped cRNA was generated by *in vitro* transcription using the T7 (for $\text{rNa}_v1.2$, $\text{rNa}_v1.3$, $\text{rNa}_v1.4$, $\text{mNa}_v1.6$, $\text{rNa}_v1.7$, and $\text{h}\beta 1$) or the SP6 (for $\text{hNa}_v1.5$, $\text{rNa}_v1.8$, and $\text{r}\beta 1$) mMESAGE mMACHINE transcription kit (Ambion, Austin, TX).

Stage V-VI oocytes were harvested by partial ovariectomy from anesthetized *Xenopus laevis* frogs as described previously (22). Oocytes were incubated in ND-96 solution (96 mM NaCl, 2 mM KCl, 1.8 mM CaCl_2 , 2 mM MgCl_2 , and 5 mM HEPES (pH 7.4)) supplemented with 50 mg/liter gentamicin sulfate and 0.5 mM theophylline. Selected oocytes were injected with cRNA at 1–3 ng/nl. Injection was conducted utilizing a microinjector (Drummond Scientific, Broomall, PA). Oocytes were stored for 1–5 days at 16 °C until sufficient expression of Na_v s was achieved.

Electrophysiology—Whole-cell currents from oocytes were recorded at room temperature (18–22 °C) by the two-electrode voltage clamp technique using a GeneClamp 500 amplifier (Molecular Devices, Sunnyvale, CA) controlled by a pClamp data acquisition system (Molecular Devices). Oocytes were placed in a bath containing ND-96 solution. Voltage and current electrodes were filled with 3 M KCl, and the resistances of both electrodes were maintained as low as possible (between 0.5 and 1.5 megaohms). The elicited currents were sampled at 20 kHz and filtered at 2 kHz using a four-pole, low pass Bessel filter. To eliminate the effect of the voltage drop across the bath grounding electrode, the bath potential was actively controlled by a two-electrode bath clamp. Leak subtraction was performed using a $-P/4$ protocol.

Whole-cell current traces were evoked every 5 s by a 100-ms depolarization to the voltage corresponding to the maximal activation of the Na_v subtype in control conditions, starting from a holding potential of -90 mV. Concentration-response curves were constructed by adding different toxin concentrations directly to the bath solution. The percentage of Na_v blockade was plotted against the logarithm of the applied concentrations and fitted with the Hill equation, $y = 100(1 + (\text{IC}_{50}/[\text{toxin}]^h)^{-1})$ where y is the percentage of block, IC_{50} is the toxin concentration at half-maximal efficacy, $[\text{toxin}]$ is the toxin concentration, and h is the Hill coefficient.

To investigate the effects on the voltage dependence of activation, current traces were induced by 100-ms depolarizations from a holding potential of -90 to 65 mV with 5-mV increments. The Na^+ conductance was calculated from the currents using Ohm's law, $g_{\text{Na}} = I_{\text{Na}}/(V - V_{\text{rev}})$ where I_{Na} is the Na^+ current peak amplitude at a given test potential V and V_{rev} is the reversal potential. The values of g_{Na} were normalized and plotted as a function of voltage and fitted using the Boltzmann equation, $g_{\text{Na}}/g_{\text{max}} = (1 + \exp((V_g - V)/k))^{-1}$ where g_{max} is the maximal g_{Na} , V_g is the voltage corresponding to half-maximal conductance, and k is the slope factor.

To investigate the effects on the steady-state inactivation process, oocytes were depolarized using a standard two-step protocol. From a holding potential of -90 mV, 100-ms pre-

Miniaturized μ -Conotoxins as Selective Na_v Blockers

pulses were generated, ranging from -90 to 65 mV with 5 -mV increments, immediately followed by a 100 -ms test pulse to -10 mV. The current amplitudes from the test pulse were normalized to the maximal Na^+ current amplitude I_{max} and plotted as a function of the applied prepulse potential using the Boltzmann equation, $I_{\text{Na}}/I_{\text{max}} = (1 + \exp(V - V_{1/2})/k)^{-1}$ where I_{max} is the maximal I_{Na} , $V_{1/2}$ is the voltage corresponding to half-maximal inactivation, V is the test voltage, and k is the slope.

Statistical analysis of the experiments was performed using a one-way analysis of variance Bonferroni test ($p < 0.05$). All data are presented as means \pm S.E. in general of at least three independent experiments ($n \geq 3$).

NMR Spectroscopy—NMR spectra were recorded with a 2 mM solution of folded Midi ($200 \mu\text{l}$) in 100% D_2O and in 80% H_2O and 20% D_2O mixtures at 5°C at 600 MHz on a Bruker Avance II 600 spectrometer equipped with a 5 -mm TCI HCN Z gradient cryoprobe. Spectra were processed using Topspin (version 2.1; Bruker Biospin) and analyzed using CARA (version 1.8.4) (24, 25).

In the one-dimensional and two-dimensional spectra in 80% H_2O , the water signal was suppressed using excitation sculpting with gradients (26). The two-dimensional NOESY in H_2O (mixing times, 150 and 300 ms) was recorded with a sweep width of 7210 Hz in both dimensions, 128 scans, 4096 data points in t_2 , and 512 free induction decays in t_1 . A two-dimensional total correlation spectroscopy spectrum in 80% H_2O with DIPSI2 sequence for mixing was recorded with a sweep width of 7210 Hz in both dimensions, 80 scans, 4096 data points in t_2 , and 512 free induction decays in t_1 (26, 27). A double quantum-filtered correlation (COSY) spectrum in H_2O was acquired using a 3 - 9 - 19 pulse sequence with gradients for water suppression allowing for presaturation during relaxation delay in cases of radiation damping (28–30).

Natural abundance ^1H , ^{13}C heteronuclear single quantum correlation in D_2O was recorded with sensitivity enhancement and gradient coherence selection optimized for selection of CH groups ($J_{\text{CH}} = 145$ Hz) using 64 scans and $256/1024$ complex data points and $30,200/6010$ Hz spectral widths in t_1 and t_2 , respectively. The two-dimensional heteronuclear single quantum correlation-total correlation spectroscopy spectrum consisted of a heteronuclear single quantum correlation building block followed by a clean MLEV-17 total correlation spectroscopy transfer step of 60 -ms mixing time just prior to the refocusing gradient with exactly the same spectral widths and number of points as heteronuclear single quantum correlation. The data were apodized with a shifted sine-bell square function in both dimensions of two-dimensional spectra.

Structural Constraints—Distance restraints were derived from NOESY spectra recorded with 150 -ms mixing times. Estimated interproton distances were derived using the isolated spin pair approximation, $r_{ij} = r_{\text{ref}} (a_{\text{ref}}/a_{ij})^{1/6}$ where r_{ij} is the estimated interproton distance, r_{ref} is the fixed internal reference distance, and a_{ref} and a_{ij} are the NOE cross-peak intensities of the reference and estimated cross-peaks, respectively. NOE interaction within geminal methylene pairs was used to determine fixed internal reference distances of 1.8 \AA . An experimental error ($\pm 20\%$) was used on the calculated interproton distances. $^3J_{\text{HNH}\alpha}$ coupling constants were measured from dou-

ble quantum-filtered COSY spectra in H_2O and then converted to dihedral restraints as follows: $^3J_{\text{HNH}\alpha} > 8$ Hz, $\varphi = -120 \pm 30^\circ$; $^3J_{\text{HNH}\alpha} < 6$ Hz, $\varphi = -60 \pm 30^\circ$.

Structure Calculations—All structure calculations were performed by means of X-PLOR-NIH V3.851 (31). A set of 100 structures was generated by torsion angle molecular dynamics, starting from an extended strand and using NMR-derived restraints. After the torsion angle molecular dynamics round (32), the majority of structures had converged to very similar structures with similar total energies and no violations of the NOE and dihedral restraints. Twenty lowest energy structures were used for further refinement during the “gentle molecular dynamics” round in explicit water (33). A box of water was constructed and optimized around selected structures obtained from torsion angle dynamics. The final refinement commenced with a 20 -ps constant temperature molecular dynamics simulation at 300 K ($20,000$ steps of 0.001 ps) and was followed by a 200 -step conjugate gradient energy minimization of the average structure of the last 10 ps of the 20 -ps simulation. Visual representations of the molecule were obtained with PyMOL Molecular Graphics System (version 1.3; Schrödinger, LLC).

RESULTS

Design Strategy

Mini Peptide—We attempted to design a chimeric, as much as possible minimized peptide benefiting from the particular characteristics of two μ -conotoxins, BuIIIC and KIIIA.

BuIIIC has recently been discovered in the venom of *C. bullatus* alongside BuIIIA and BuIIIB (21). Strikingly, they differ greatly from previously isolated μ -conotoxins because they only contain three residues in the second intercysteine loop as opposed to four (Table 1A). BuIIIC demonstrates a strong block on $\text{Na}_v1.4$ (96% at $1 \mu\text{M}$) (21). We retained the structural characteristics as well as its potent block.

An additional μ -conotoxin gaining our interest was KIIIA because it is the smallest μ -conotoxin identified thus far, containing 16 AAs (20). Its short first intercysteine loop contains but one Asn residue, whereas other μ -conotoxins possess at least three or even eight residues in this loop (Table 1A).

For construction of the chimeric Mini peptide, residues of the three intercysteine loops were taken into consideration as “building blocks.” The first loop is based on KIIIA and contains an Asn residue. For the second loop, we considered the sequences of BuIIIA, BuIIIB, and BuIIIC. BuIIIA and BuIIIB incorporate Gly-Arg-Trp, whereas BuIIIC encompasses the sequence Ser-Arg-Trp. A considerably larger number of μ -conotoxins bear at least one Ser residue in the second loop (Table 1A, 12 of 18). This proves to be a more favorable residue from an evolutionary viewpoint rather than Gly (Table 1A, six of 18). Hence the sequence of BuIIIC was selected to construct the second loop. Concerning the third loop, BuIIIC and KIIIA contain identical residues. In addition, comparable sequences are found in other μ -conotoxins (e.g. SIIIA, SmIIIA, and CIIIA; Table 1A). Therefore, these BuIIIC/KIIIA residues were incorporated in the chimeric peptide.

We integrated recent results by Han *et al.* (34) into our design strategy. They illustrated that the first disulfide bridge between

TABLE 1
Sequences of naturally occurring μ -conotoxins and synthetically designed peptides

Shown are the sequences of the 19 known, naturally occurring μ -conotoxins (A), the two naturally occurring peptides KIHA and BuIIIC from which the Mini peptide was derived and the artificially designed Mini peptide (B), and the three series of synthetic derivatives (C). Dashes are put in the sequences to make all sequences and inter-cysteine loops of comparable length. "AAs" represents the total number of residues. The first sequence of all series is the sequence of the peptide from which the series is derived (e.g. the Mini peptide or Midi peptide). Residue numbers are indicated below the corresponding sequences. Black lines above the sequences, disulfide bridges; asterisks, deletions of Cys residues; red amino acids, changes as compared with the sequence of the Mini peptide (Series 1) or with the Midi peptide (Series 2 and 3); number sign (#), C-terminal amidation; Z, pyroglutamate; O, hydroxyproline. AAs in gray lie in the first inter-cysteine loop, AAs in turquoise lie in or are derived from the second inter-cysteine loop, and AAs in green lie in or are derived from the third inter-cysteine loop.

A. μ -Conotoxin	Sequence	AAs	Cone snail	Ref.
KIHA	---CCN-----C SSKW CRDHSRCC	# 16	<i>Conus kinoshitai</i>	(20)
SIIIA	ZN--CCN-----GGC SSKW CRDHARCC	# 20	<i>Conus striatus</i>	(20)
SIIIB	ZN--CCN-----GGC SSKW CKGHARCC	# 20	<i>Conus striatus</i>	(37)
PIIA	ZRL--CCG---FOK SCRSRQ CKOH--RCC	# 22	<i>Conus purpurascens</i>	(49)
GIIIA	-RD--CCT---O OKK CKDR Q CKO Q --RCCA	# 22	<i>Conus geographus</i>	(50)
GIIIB	-RD--CCT---O OKK CKDR R CKO M --KCCA	# 22	<i>Conus geographus</i>	(50)
GIIIC	-RD--CCT---O OKK CKDR R CKO L --KCCA	# 22	<i>Conus geographus</i>	(50)
TIIIA	-RHGC CK ---G OKGC SSRE CROQ --HCC	# 22	<i>Conus tulipa</i>	(51)
SmIIIA	ZR--CCN---GRRGC SSRW CRDHSRCC	# 22	<i>Conus stercusmuscarum</i>	(52)
CIIIA	GR--CCE---GPNGC SSRW CKDHARCC	# 22	<i>Conus catus</i>	(53)
MIIIA	ZG--CCN---VPNGC SGRW CRDHAQCC	# 22	<i>Conus magus</i>	(53)
CnIIIA	GR--CCD---VPNAC SGRW CRDHAQCC	# 22	<i>Conus consors</i>	(53)
CnIIIC	ZG--CCN---GPKGC SSKW CRDHARCC	# 22	<i>Conus consors</i>	(54)
SxIIIA	---RCCT--G KKG SGR AC KNL--KCCA	# 22	<i>Conus striolatus</i>	(55)
BuIIIA	-TDR CK ---G KREC --GRWCRDHSRCC	# 22	<i>Conus bullatus</i>	(21)
SxIIIB	ZK--CCT--G KKG SGR AC KNL--RCCA	# 23	<i>Conus striolatus</i>	(55)
BuIIIB	VGER CKN --G KRGC --GRWCRDHSRCC	# 24	<i>Conus bullatus</i>	(21)
CnIIIB	ZG--CCG---EPN LCFTRW CRNNARCC RQ	25	<i>Conus consors</i>	(53)
BuIIIC	IVDR CCNKGN GK RGC --SRWCRDHSRCC	# 26	<i>Conus bullatus</i>	(21)
B. Mini peptide				
KIHA	---CCN-----C SSKW CRDHSRCC	# 16		
BuIIIC	IVDR CCNKGN GK RGC --SRWCRDHSRCC	# 26		
Mini	---*CN-----C-- SRW *RDHSRCC	# 13		
C. Series 1				
Mini	---CN-----C-- SRW --RDHSRCC	# 13		
R5A-Mini	---CN-----C-- SAW --RDHSRCC	# 13		
R5E-Mini	---CN-----C-- SEW --RDHSRCC	# 13		
Extra-Mini	---CN-----C--* RW --RDHSRCC	# 12		
Midi	---CN-----C-- SRWA RDHSRCC	# 14		
Series 2				
Midi	---CN-----C-- SRWA --RDHSRCC	# 14		
EAD-Midi	--- ECN -----C-- SRWA -- RAHSRCCD	# 16		
EAK-Midi	--- ECN -----C-- SRWA -- RAHSRCCK	# 16		
AA-Midi	---CN-----C-- SRWA A RDHSRCC	# 15		
Series 3				
Midi	---CN-----C-- SRWA RDHSRCC	# 14		
R1-Midi	--- CR -----C-- SRWA RDHSRCC	# 14		
R2-Midi	---CN-----C-- RRWA RDHSRCC	# 14		
R3-Midi	---CN-----C-- SRWA R SRCC	# 14		

Cys¹ and Cys⁹ in KIHA is removable, almost without affecting the original activity of the peptide on $\text{Na}_v1.2$ and $\text{Na}_v1.4$ (34). Ultimately, the first disulfide bridge was excluded in our chimeric pep-

ptide. The resulting peptide was named "Mini peptide" by reason of its sequence of only 13 AAs (Table 1B). This renders the Mini peptide even shorter than the smallest μ -conotoxin known to date.

TABLE 2

Comparison of activities of Mini and analogues with other μ -conotoxinsPercentages of block are given as \pm S.D. —, not determined for that isoform.

	Concentration	$\text{Na}_v1.2$	$\text{Na}_v1.4$	Ref.
BuIIIC	1 μM	—	96	21
KIIIA	1 μM	90 \pm 3.3	86 \pm 5.6	35
KIIIA(K7A)	1 μM	80 \pm 5.9	32 \pm 5.7	35
KIIIA(C1A,C9A)	1 μM	93 \pm 2.0	85 \pm 2.0	34
Mini	20 μM	63.3 \pm 4.9	46.6 \pm 1.8	This study
Midi	1 μM	88.8 \pm 2.0	83.3 \pm 2.4	This study
R1-Midi	1 μM	91.23 \pm 0.5	74.4 \pm 1.3	This study
R2-Midi	1 μM	95.5 \pm 0.7	76.6	This study

First Series of Analogues—Its short sequence makes the Mini peptide an interesting starting point for further structure-function optimization. Therefore, three series of peptides were developed based on the Mini peptide (overview in Table 1C). In a research study, Zhang *et al.* (35) nicely demonstrated the importance of several residues in KIIIA by means of an alanine scan. The original KIIIA peptide has a slight preference for the $\text{Na}_v1.2$ over the $\text{Na}_v1.4$ isoform (Table 2) (22). One of the analogues that was tested in the study, KIIIA(K7A), strongly influenced the discrimination between $\text{Na}_v1.2$ and $\text{Na}_v1.4$ (Table 2). We integrated this in our design strategy, resulting in the two analogues Mini-R5A and Mini-R5E. A third peptide was based on results of Han *et al.* (34). They established that the adjacent Ser⁵ and Ser⁶ in KIIIA could be replaced by a PEG backbone without severely affecting the block on $\text{Na}_v1.2$ (Table 2). This prompted us to hypothesize that Ser⁴ in the Mini peptide may also be excluded. The resulting peptide was named Extra-Mini as it contained only 12 AAs. The last peptide in this series was named Midi peptide and comprised one extra Ala. It was incorporated where initially the third Cys residue was removed in KIIIA/BuIIIC. This was conducted to restore the appropriate spacing as we suspected spacing to be important for the correct formation of the α -helix (36) (Table 1C, Series 1).

Second Series of Analogues—Because the Midi peptide of Series 1 exhibited the best results of all tested peptides (see “Electrophysiological Characterization”), we started from this sequence in developing the second series of peptides. In EAD-Midi and EAK-Midi, a negative charge was removed in the third loop; instead, a neutralizing Ala was incorporated. This was done in accordance with results of Schroeder *et al.* (37), who demonstrated that removing Asp¹⁵ in SIIIA (*Conus striatus*) caused a 10-fold increase in $\text{Na}_v1.2$ affinity, resulting in a 70-fold neuronal selectivity of $\text{Na}_v1.2$ over $\text{Na}_v1.4$. We combined this with the addition of extra C- and N-terminal residues to examine the influence of positive or negative charges. N-terminally, an extra Glu was integrated. C-terminally, an extra Asp providing a negative charge or a Lys providing a positive charge was incorporated (Table 1C, Series 2). Finally, to further explore the effects of spatial distance in the Midi peptide, one extra Ala was integrated in the Midi sequence immediately next to the first extra Ala. This gave rise to AA-Midi (Table 1C, Series 2).

Third Series of Analogues—The Midi peptide acted once more as our starting point for the third series of peptides. This series was based on the general knowledge that basic residues are important for binding of μ -conotoxins (38, 39). Likewise,

the analog SIIIA(H16R) was 137 times more selective for the neuronal $\text{Na}_v1.2$ isoform compared with $\text{Na}_v1.4$ (37). We endeavored to obtain a similar selectivity profile by replacing His¹⁰ with an Arg in the Midi peptide. Furthermore, we investigated the effect of introducing similar mutations in the first and second loops and altered Asn² and Ser⁴ individually into Arg. The resulting peptides were named R1-Midi, R2-Midi, and R3-Midi (Table 1C, Series 3).

Folding of Mini and Analogues

To investigate the folding of the Mini peptide, changes in HPLC retention time were followed and compared with the retention time of the reduced peptide (supplemental Fig. S1). When the first folding strategy was used, folding was rather slow and resembled the slow rearrangement folding of GIIIA from *Conus geographus* (23). HPLC profiles of aliquots quenched at 30 s, 30 min, 60 min, and 24 h displayed minor accumulation of the folded Mini peptide. Only after 1 week was a clear accumulation of folded peptide observed with minor traces of the non-folded forms. After 1 month, the HPLC profile did not differ significantly from that witnessed after 1 week, suggesting that folding reached a maximum after 1 week. The second folding strategy rather resulted in a rapid collapse pattern and reached a maximum after 30 min (supplemental Fig. S1). This is comparable with the folding of PIIIA (*Conus purpurascens*) and SmIIIA (*Conus stercus-muscarum*) (23). To confirm folding, HPLC peaks were freeze-dried and analyzed by means of electrospray ionization MS. The corresponding molecular masses indicated that the Mini peptide was folded (monoisotopic mass, 1621.8 Da; calculated mass, 1620.8 Da). For all analogues of the Mini peptide, the second method was used as folding strategy (data not shown).

Electrophysiological Characterization

Mini Peptide—The effects of the Mini peptide were evaluated on a series of Na_v isoforms expressed in *X. laevis* oocytes. The Mini peptide reduced the peak Na^+ current in all tested isoforms. At 20 μM , the largest block was seen on $\text{Na}_v1.2$ (63.3 \pm 4.9%) followed by $\text{Na}_v1.4$ (46.6 \pm 1.8%) and $\text{Na}_v1.6$ (37.9 \pm 3.9%). A minor effect was noticed on $\text{Na}_v1.5$ (15.4 \pm 2.7%), $\text{Na}_v1.7$ (19.9 \pm 4.3%), and $\text{Na}_v1.8$ (17.3 \pm 4.2%). On $\text{Na}_v1.3$, a median effect was established (36.6 \pm 3.7%) (Fig. 1).

Series 1—R5E-Mini, R5A-Mini, and Extra-Mini exhibited a minor to no block on $\text{Na}_v1.2$, $\text{Na}_v1.4$, and $\text{Na}_v1.6$ at 75 nM (Fig. 2, Series 1). Only concentrations starting from 10 μM were able

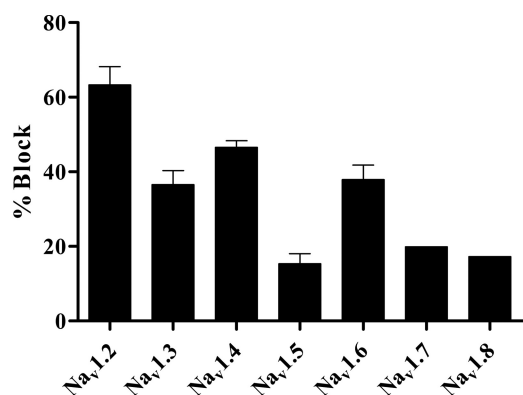


FIGURE 1. Block of different Na_v isoforms by 20 μM Mini peptide. Currents from voltage-clamped *X. laevis* oocytes were measured as described under "Experimental Procedures." The Mini peptide was tested on $\text{Na}_v1.2$ – $\text{Na}_v1.8$. Mean percentages of block are calculated for each isoform for at least three experiments (for $\text{Na}_v1.7$ and $\text{Na}_v1.8$, $n = 2$), and S.E. is indicated by error bars, if appropriate. Mini preferentially blocks $\text{Na}_v1.2$ (63.3 \pm 4.9%) over $\text{Na}_v1.4$ (46.6 \pm 1.8%) and $\text{Na}_v1.6$ (37.9 \pm 3.9%), respectively. Percentages of block were as follows for other isoforms (mean \pm S.E.): $\text{Na}_v1.3$, 36.6 \pm 3.7%; $\text{Na}_v1.5$, 15.4 \pm 2.7%; $\text{Na}_v1.7$, 19.9 \pm 4.3%, and $\text{Na}_v1.8$, 17.3 \pm 4.2%.

to induce a small block on these three isoforms (data not presented). The Midi peptide in contrast displayed a major block of 52.2 \pm 1.2% on $\text{Na}_v1.2$ at 75 nM. Consequently, blocking characteristics of the Midi peptide were further examined, and concentration-response curves were fitted (Fig. 3A). IC_{50} values were 77.8 \pm 5.9 nM for $\text{Na}_v1.2$, 53.4 \pm 2.0 nM for $\text{Na}_v1.4$, 2373.1 \pm 94.1 nM for $\text{Na}_v1.5$, and 115.7 \pm 27.4 nM for $\text{Na}_v1.6$. $\text{Na}_v1.3$ and $\text{Na}_v1.5$ could only be blocked with concentrations starting from 100 nM. When a concentration of 10 μM was used, both isoforms were blocked around 40%. As such, the corresponding IC_{50} values are of relative meaning, and represented concentration-response curves are only based on the available data up to 10 μM .

Series 2—Unfortunately, all three peptides of the second series (EAD-Midi, EAK-Midi, and AA-Midi) exhibited minor to no block on $\text{Na}_v1.2$ at a concentration of 75 nM (less than 5%; Fig. 2, Series 2). The block only started from concentrations in the micromolar range. The equivalent was observed for isoforms $\text{Na}_v1.4$ and $\text{Na}_v1.6$ where the block also only started at micromolar concentrations (data not presented).

Series 3—The last series of peptides comprises R1-Midi, R2-Midi, and R3-Midi. R1-Midi had an activity profile comparable with the Midi peptide. Likewise, it offered a comparable inhibition of the current of $\text{Na}_v1.2$ at 75 nM. R3-Midi presented a somewhat weaker inhibition (only 37.0 \pm 5.7%). R2-Midi on the contrary displayed a large block on $\text{Na}_v1.2$, and thus, R2-Midi appeared to be the most potent blocker of all peptides tested (Fig. 2, Series 3). A concentration-response curve for R2-Midi was constructed for $\text{Na}_v1.2$, yielding an IC_{50} value of 34.1 \pm 0.01 nM (Fig. 3B).

Comparison of the Effects of the Three Most Interesting Peptides

When comparing the effects of 75 nM Midi on different isoforms, it was observed that Midi blocked $\text{Na}_v1.2$ to a similar extent as $\text{Na}_v1.4$ (52.2 versus 51.7%, respectively) followed by $\text{Na}_v1.6$ (41.2%). The isoforms $\text{Na}_v1.3$, $\text{Na}_v1.5$, and $\text{Na}_v1.8$ were not blocked by Midi at 75 nM (Fig. 4). R1-Midi, however, made

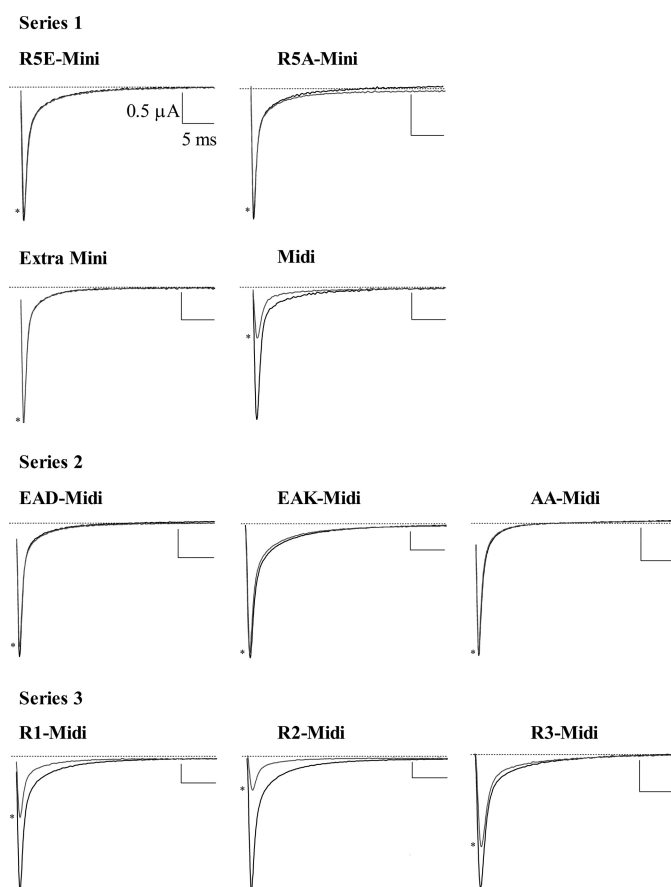


FIGURE 2. Representative current traces of all peptides of Series 1, 2, and 3 at 75 nM on $\text{Na}_v1.2$. Traces were obtained by two-electrode voltage clamp on *X. laevis* oocytes expressing the $\text{Na}_v1.2$ isoform as described under "Experimental Procedures." Currents were evoked by a depolarizing pulse starting from a holding potential of -90 mV to the voltage corresponding to the maximal activation in control conditions. Asterisks indicate the steady-state peak amplitude of the currents after exposure to the toxins. Because the Mini peptide preferentially blocked $\text{Na}_v1.2$, this isoform was chosen to illustrate representative blocking activities of the other series. The most potent blockers are Midi (traces represented here; 52.88% of block), R1-Midi (54.32% of block), and R2-Midi (70.9% of block). Scale bars, 5 ms for horizontal lines and 0.5 μA for vertical lines.

a clear distinction between $\text{Na}_v1.2$ (56.0 \pm 1.9%) over $\text{Na}_v1.4$ (39.7 \pm 2.6%) and $\text{Na}_v1.6$ (only 22.5 \pm 2.5%). R2-Midi displayed the largest block of all three peptides on $\text{Na}_v1.2$ (70.3 \pm 2.4%). Furthermore, 75 nM R2-Midi exhibited a block of 45.5 \pm 0.7% on $\text{Na}_v1.4$ and 45.5 \pm 1.1% on $\text{Na}_v1.6$ (Fig. 4).

When a one-way analysis of variance Bonferroni statistical analysis was performed on these results, Midi differed significantly for $\text{Na}_v1.2$ compared with the other isoforms ($p < 0.05$). However, the block was not significantly different for $\text{Na}_v1.2$ compared with $\text{Na}_v1.4$. The same holds true for $\text{Na}_v1.3$ against $\text{Na}_v1.5$ and $\text{Na}_v1.8$ ($p > 0.05$). The effects of R1-Midi differed significantly for $\text{Na}_v1.2$ set against all other isoforms ($p < 0.05$). For $\text{Na}_v1.3$, $\text{Na}_v1.5$, and $\text{Na}_v1.8$, no significant differences were observed. For R2-Midi, comparable degrees of block were noticed on $\text{Na}_v1.4$ and $\text{Na}_v1.6$ and on $\text{Na}_v1.5$ and $\text{Na}_v1.8$ ($p > 0.05$). Interestingly, the residual currents on $\text{Na}_v1.2$ displayed by R1-Midi (9.8 \pm 0.5%) and R2-Midi (4.5 \pm 0.7%) were somewhat larger than the residual current displayed by Midi itself (1.2 \pm 1.1%).

Miniaturized μ -Conotoxins as Selective Na_v Blockers

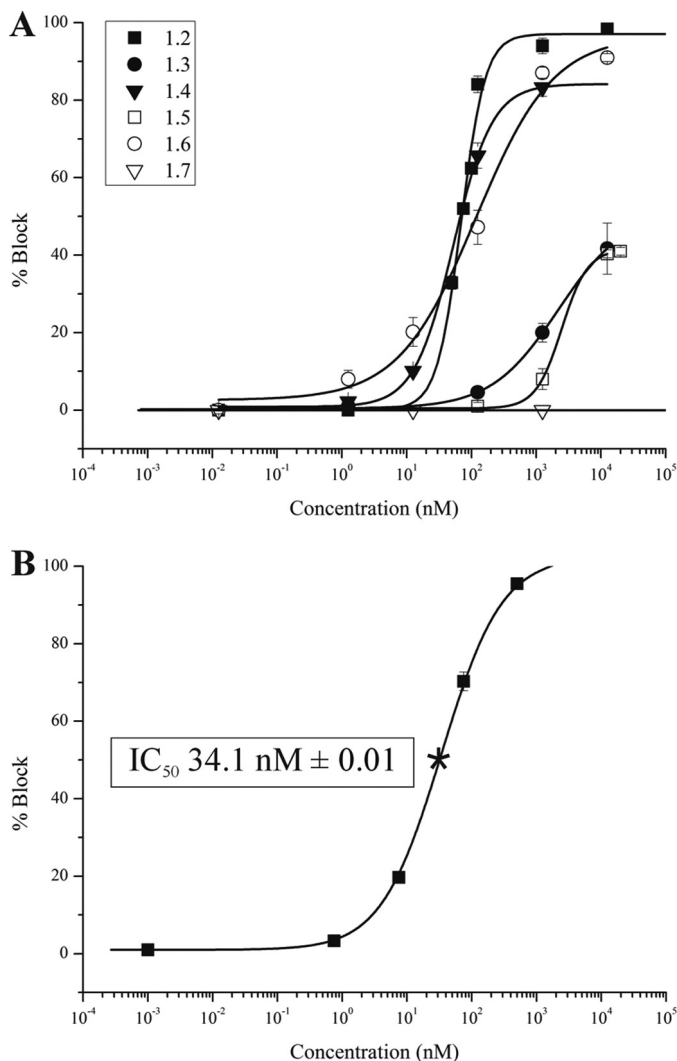


FIGURE 3. Concentration-response curves for the Midi peptide and R2-Midi. *A*, Midi was tested in different concentrations on a range of isoforms to obtain the corresponding IC_{50} values. *B*, R2-Midi was tested in different concentrations on $\text{Na}_v1.2$. The asterisk indicates the IC_{50} value of R2-Midi on $\text{Na}_v1.2$, being $34.1 \text{ nM} \pm 0.01$. Currents were obtained as described under "Experimental Procedures." The percentage of block was plotted against the logarithm of the tested concentrations. For all Na_v isoforms, results were fit with the Hill equation. IC_{50} values of the Midi peptide were $77.8 \pm 5.9 \text{ nM}$ for $\text{Na}_v1.2$, $53.4 \pm 2.0 \text{ nM}$ for $\text{Na}_v1.4$, $2373.1 \pm 94.1 \text{ nM}$ for $\text{Na}_v1.5$, and $115.7 \pm 27.4 \text{ nM}$ for $\text{Na}_v1.6$. IC_{50} values for $\text{Na}_v1.3$ and $\text{Na}_v1.5$ are of relative meaning as they are only blocked by concentrations starting from 100 nM .

Kinetics and Voltage Dependence of Block

To investigate the reversibility of block and determine kinetics of block of Midi, R1-Midi, and R2-Midi, washouts were conducted on $\text{Na}_v1.2$. For all peptides, the block could be reversed, albeit often very slowly. Therefore, exact kinetics of block could not be determined. Effects on the voltage dependence of activation and steady-state inactivation were analyzed for Midi and R2-Midi on $\text{Na}_v1.2$. No shifts were observed in the activation and steady-state inactivation curves of Midi and R2-Midi (supplemental Fig. S2).

NMR Spectroscopy

The solution structure of the Midi peptide was determined by NMR spectroscopy. The quality of the calculated structure

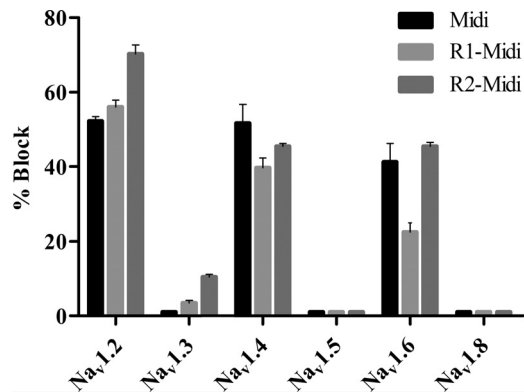


FIGURE 4. Overview of block by Midi, R1-Midi, and R2-Midi. The three peptides were tested on $\text{Na}_v1.2$, $\text{Na}_v1.3$, $\text{Na}_v1.4$, $\text{Na}_v1.5$, $\text{Na}_v1.6$, and $\text{Na}_v1.8$ at a concentration of 75 nM . When no block is seen at that concentration, this is represented by an arbitrary value of 1% for the clarity of the figure. This is the case for Midi on $\text{Na}_v1.3$, $\text{Na}_v1.5$, and $\text{Na}_v1.8$ and for R1-Midi and R2-Midi on $\text{Na}_v1.5$ and $\text{Na}_v1.8$. Other specific values are discussed under "Results." Data are represented as the means \pm S.E. (indicated by error bars); each experiment was performed at least three times ($n \geq 3$).

TABLE 3

Structure statistics of the Midi peptide derived from NMR structural analysis

r.m.s.d., root mean square deviation.

Quantity	Value
Total unambiguous distance restraints	179
Intraresidual	128
Sequential ($ i - j = 1$)	34
Medium ($2 \leq i - j \leq 4$)	10
Long range ($ i - j \geq 5$)	7
Dihedral angles	29
r.m.s.d. from the average atomic coordinates (\AA)	
Backbone (N, C $^\alpha$, C $^\gamma$)	3.41 ± 1.67
Heavy atoms	2.63 ± 1.31
Deviation from idealized covalent geometry	
Bond (\AA)	0.0006 ± 0.0000
Angles ($^\circ$)	2.882 ± 0.085
Improper ($^\circ$)	2.323 ± 0.521
Ramachandran analysis (%)	
Residues in most favored regions	49.6
Residues in additional allowed regions	49.6
Residues in generously allowed regions	0.8
Residues in disallowed regions	0

was evaluated by means of the root mean square deviation values from the average structure (Table 3). The Midi peptide adopted a flexible structure without the typical α -helix observed in μ -conotoxins (Fig. 5A). Its N- and C-terminal regions differed greatly from the corresponding regions in KIIIA(C1A,C9A) in which the same disulfide bridge was removed as for the Midi peptide. However, some key basic residues appeared to be distributed in a manner similar to that in KIIIA(C1A,C9A) (Fig. 5B). Models of KIIIA(C1A,C9A) were generated using the solution structure deposited in the BioMagResBank (accession number 20049) by Khoo *et al.* (36). The solution structure of the Midi peptide was deposited in the Protein Data Bank under code 2LU6.

DISCUSSION

In current study, we demonstrate a successful strategy to design small subtype-selective compounds. A series of 11 peptides were developed, all of which established a block on Na_v s. The initial Mini peptide demonstrated activities at micromolar

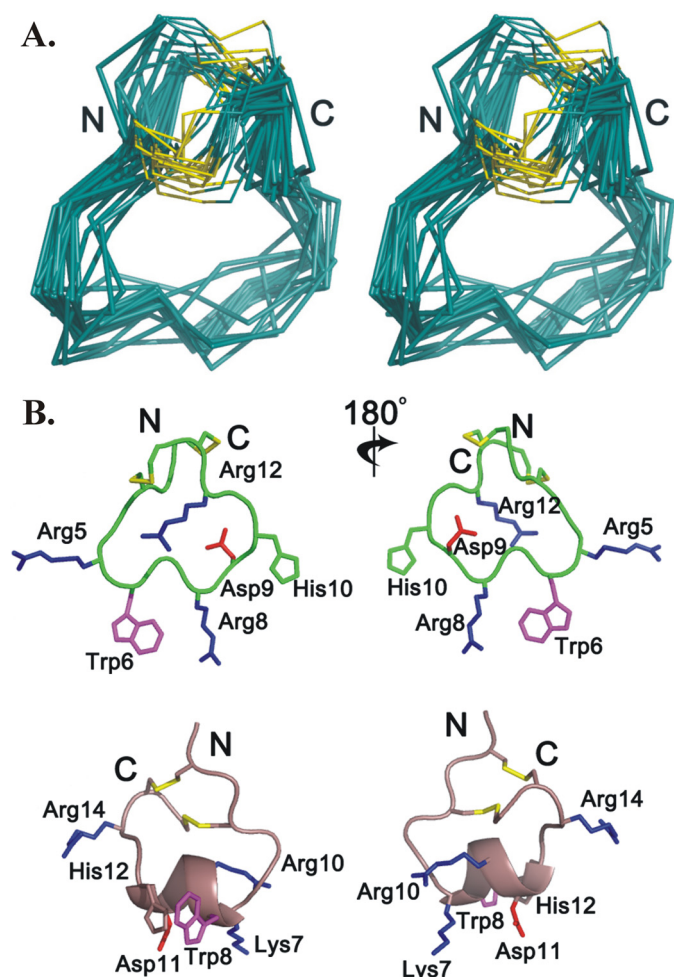


FIGURE 5. NMR structure of the Midi peptide. A, stereoviews of a family of 20 final structures of the Midi peptide superimposed over backbone heavy atoms (N, C $^{\alpha}$, and C $^{\beta}$) with disulfide bonds colored gold. B, front and back views of the closest-to-average structure of the Midi peptide (top) and KIIIA(C1A,C9A) where the first disulfide bridge is removed (bottom) with side chain heavy atoms of key residues displayed and labeled. Disulfide bridges are colored gold, positively charged residues are red, negatively charged residues are blue, hydrophilic residues are green, and aromatic residues are magenta. The two views are related by a 180° rotation around the vertical axis.

concentrations. KIIIA and Mini have identical selectivity profiles, and both block $\text{Na}_v1.2$ to a larger extent than $\text{Na}_v1.4$ (Table 2) followed by $\text{Na}_v1.6$ (35, 36). This might in part be caused by the presence of a Trp residue (Trp⁶ in Mini and Trp⁸ in KIIIA) as suggested previously (22, 35).

An extra Ala residue added to the sequence of the Mini peptide to restore the spacing (in comparison with the original μ -conotoxins) led to a peptide active in nanomolar concentrations. This may imply that the difference in biological activity of Mini (in a micromolar range) and Midi (in a nanomolar range) can be due to a difference in spacing and that at least six residues are required to set up a fully functional bioactive scaffold that can interact properly with a binding area on the Na_v channel (37). Interestingly, an α -helix does not appear to be strictly necessary for the biological activity of μ -conotoxins because this structure was not identified within the Midi peptide as defined by NMR. In KIIIA, this α -helix is situated between Lys⁵ and His¹² (36).

KIIIA and Midi exhibit comparable potencies with IC₅₀ values on $\text{Na}_v1.2$, $\text{Na}_v1.4$, and $\text{Na}_v1.6$ around nanomolar concentrations (22). Notwithstanding the nearly complete block on $\text{Na}_v1.4$ by BuIIIC at 1 μM , Midi demonstrated a smaller block on $\text{Na}_v1.4$ at the same concentration (Table 2). Moreover, the block is only complete at a 10-fold higher concentration. Possibly, the bulky structure of BuIIIC (27 AAs) allows a more complete occlusion of the Na^+ conduction pathway at lower concentrations. Besides a larger steric hindrance of Na^+ ions for BuIIIC, additional positive charges in BuIIIC can cause a larger electrostatic repulsion than for the Midi peptide. The mutant R2-Midi in which an extra positive charge also leads to lower IC₅₀ values confirms this hypothesis, which was also proposed previously (40).

Spacing is important for the activity of the Midi peptide. However, this also applies to the Extra-Mini peptide in which Ser⁴ was additionally eliminated. Our results indicate that this distorts the formation of a bioactive scaffold. This probably hinders the appropriate binding of its key residues to the Na_v channel. Once Arg⁵ in Mini was replaced either by an Ala resulting in Mini-R5A or by a Glu resulting in Mini-R5E, activities were also severely affected. This concurs with previous studies in which the corresponding Arg was suggested to be determinant for block of $\text{Na}_v1.2$ and $\text{Na}_v1.4$ (35, 37, 41).

For the second series of peptides, additional N- and C-terminal residues were added to the sequence of Midi. This was combined with modification of Asp⁹ into Ala. Our results do not correspond to those of Schroeder *et al.* (37). They demonstrated that replacement of the corresponding Asp¹⁵ in SIIIA led to a more selective $\text{Na}_v1.2$ block. For our peptides EAD-Midi and EAK-Midi, blocking activity was nonetheless seriously affected. However, our results correspond partially to those obtained for an analog of KIIIA. When Asp¹¹ in KIIIA was replaced by Ala, this caused a small reduction in block of 5% for $\text{Na}_v1.2$ and a large reduction in block of 45% for $\text{Na}_v1.4$ (calculated from data of Ref. 35). In the EAD- and EAK-Midi peptides, the simultaneous introduction of three mutations at once was probably a deleterious combination.

The final series of peptides provided us with interesting data concerning the role of basic residues in the interactions of μ -conotoxins with Na_v channels. The importance of basic residues in the binding of the μ -conotoxins with Na_v channels has been established previously. Residue Arg¹³ of GIIIA has been one of the most intensively studied residues in this respect. It was established to bind to a negative charge (Glu⁷⁵⁸) in DII of $\text{Na}_v1.4$ (42). Likewise, interactions were demonstrated between Arg¹⁹ of GIIIA and residues Asp⁷⁶² and Glu⁷⁶⁵ in the P-S6 loop of DII of $\text{Na}_v1.4$ (43). Based on the potent block of R1-Midi and R2-Midi on $\text{Na}_v1.2$, $\text{Na}_v1.4$, and $\text{Na}_v1.6$, it can be stated that basic amino acids are key residues for a strong binding of the peptide to the channel (Fig. 4). Nevertheless, the most striking compound in this series is undoubtedly R2-Midi because this compound exhibits a very potent and selective block on $\text{Na}_v1.2$. Consequently, this makes R2-Midi an interesting compound for development as a therapeutic agent in $\text{Na}_v1.2$ -related diseases such as epilepsy.

As demonstrated for KIIIA (22), SIIIA (15), PIIIA (41), and certain derivatives of GIIIA (40), the block was never complete

for any of the peptides that could be tested at their maximum concentrations (e.g. Midi, R1-Midi, and R2-Midi). Charge-neutralizing substitutions at three positions in PIIIA also caused a residual current. It was suggested that its basic residues interact with channel residues close to the Na^+ conduction pathway. Thereby, the pore of the channel is blocked electrostatically or sterically (41). However, this toxin-channel interaction could allow some Na^+ ions or even tetrodotoxin to sneak by, causing a residual current (12, 16, 24, 40). A small residual current was similarly observed for derivatives of GIIIA at one single position (Arg¹³). Nonetheless, following this reasoning, R1-Midi and R2-Midi should cause more electrostatic repulsion compared with Midi due to the addition of a positive Arg. Their residual currents should be smaller as opposed to those of the Midi peptide. However, this is not the case. Possibly, there are supplementary, non-electrostatic components that contribute to the mechanism of block observed for R1-Midi and R2-Midi. Recently, it was proven by molecular dynamic simulations for PIIIA that differences in binding affinity on $\text{Na}_v1.4$ can be due to a slightly different location of binding in the pore region. One of its structural isomers was simulated to bind to a region located deeper in the pore, correlating to a higher binding affinity on $\text{Na}_v1.4$ (44). Consequently, small differences in binding affinities reveal that our μ -conotoxin derivatives bind at slightly different regions, although all located in the pore and therefore leading to block of Na^+ conduction.

Interestingly, our NMR data indicate that Midi adapts a rather flexible structure devoid of an α -helix. All $^3J_{\text{HNH}\alpha}$ coupling constants extracted from double quantum-filtered COSY spectra (measured at 5 °C; data not displayed) are between 6 and 8 Hz, indicative of a very flexible structure. Despite the lack of an α -helix, the Midi peptide blocks Na_v s at nanomolar concentrations. This is in accord with recent studies of an isomer of PIIIA that also had a flexible conformation but remained active on $\text{Na}_v1.4$ (44). Apparently, an α -helix is not strictly essential to acquire a fully active peptide. Possibly, some of the basic residues incorporated in the Midi peptide are distributed in a manner close to the arrangement in KIIIA(C1A,C9A) (Fig. 5B), leading to a similar activity profile. Further evidence is presented by Chen and Chung (45), who suggest that PIIIA may block the Na_v with various binding modes. Different basic residues can thereby all protrude into the selectivity filter and block the pore, whereas other residues can make electrostatic contacts at the outer vestibule of the channel. Because the basic residues of Midi are also symmetrically distributed, this allows the peptide to form multiple binding modes with the Na_v channel. It will be interesting to generate molecular dynamics simulations for Midi as well.

For a peptide to be eligible for development as a therapeutic compound, it is essential that it remains stable *in vivo*. To improve stability, cyclic peptides or lactam-stabilized peptides can be formed (46). This can for instance be achieved by means of native chemical ligation (for a review, see Ref. 47). Regardless, whether these modifications do not influence the activities of the peptides and whether they still exhibit the same potencies as the original peptides need be determined.

With our results, we prove that it is possible to design very small peptides based on known pharmacophores of μ -conotox-

ins without losing their potency and therapeutically important selectivity. We confirm that removal of one disulfide bridge does not affect their activity. By defining the NMR structure of the Midi peptide, we deliver evidence that the α -helical structure that has traditionally been considered as responsible for the biological activity of μ -conotoxins is not strictly necessary. Finally, we demonstrate that it is possible to obtain more selective peptides by thoughtfully mutating particular amino acids in the sequence of μ -conotoxins. Therefore, our miniaturized compounds are an ideal starting platform in the pursuit of novel therapeutics that can be used to treat Na_v -related diseases such as epilepsy (48) and pain (34, 35).

Acknowledgments—We thank A. L. Goldin (University of California, Irvine, CA) for sharing r $\text{Na}_v1.2$, r $\text{Na}_v1.3$, and m $\text{Na}_v1.6$; G. Mandel (Stony Brook University, Stony Brook, NY) for sharing r $\text{Na}_v1.4$; R. G. Kallen (University of Pennsylvania, Philadelphia, PA) for sharing h $\text{Na}_v1.5$; P. Dietrich (Roche Applied Science) for sharing r $\text{Na}_v1.7$; J. N. Wood (University College, London, UK) for sharing r $\text{Na}_v1.8$; S. H. Heinemann (Friedrich-Schiller-Universität, Jena, Germany) for sharing the r $\beta 1$ subunit; and S. C. Cannon (University of Texas, Dallas, TX) for sharing the h $\beta 1$ subunit. We are also grateful to Elia Diego-García, Bert Billen, Annelies Van Der Haegen, and Sarah Debaveye for helpful discussions and/or technical assistance and to Nick Van Nuffelen for carefully proofreading this manuscript.

REFERENCES

- Escayg, A., and Goldin, A. L. (2010) Sodium channel SCN1A and epilepsy: mutations and mechanisms. *Epilepsia* **51**, 1650–1658
- Jurkat-Rott, K., Holzherr, B., Fauler, M., and Lehmann-Horn, F. (2010) Sodium channelopathies of skeletal muscle result from gain or loss of function. *Pflugers Arch.* **460**, 239–248
- Campuzano, O., Beltrán-Alvarez, P., Iglesias, A., Scornik, F., Pérez, G., and Brugada, R. (2010) Genetics and cardiac channelopathies. *Genet. Med.* **12**, 260–267
- Mantegazza, M., Curia, G., Biagini, G., Ragsdale, D. S., and Avoli, M. (2010) Voltage-gated sodium channels as therapeutic targets in epilepsy and other neurological disorders. *Lancet Neurol.* **9**, 413–424
- Shon, K. J., Grilley, M. M., Marsh, M., Yoshikami, D., Hall, A. R., Kurz, B., Gray, W. R., Imperial, J. S., Hillyard, D. R., and Olivera, B. M. (1995) Purification, characterization, synthesis, and cloning of the lockjaw peptide from *Conus purpurascens* venom. *Biochemistry* **34**, 4913–4918
- Buczek, O., Wei, D., Babon, J. J., Yang, X., Fiedler, B., Chen, P., Yoshikami, D., Olivera, B. M., Bulaj, G., and Norton, R. S. (2007) Structure and sodium channel activity of an excitatory II-superfamily conotoxin. *Biochemistry* **46**, 9929–9940
- McIntosh, J. M., Hasson, A., Spira, M. E., Gray, W. R., Li, W., Marsh, M., Hillyard, D. R., and Olivera, B. M. (1995) A new family of conotoxins that blocks voltage-gated sodium channels. *J. Biol. Chem.* **270**, 16796–16802
- Spence, I., Gillissen, D., Gregson, R. P., and Quinn, R. J. (1977) Characterization of the neurotoxic constituents of *Conus geographus* (L.) venom. *Life Sci.* **21**, 1759–1769
- Terlau, H., and Olivera, B. M. (2004) *Conus* venoms: a rich source of novel ion channel-targeted peptides. *Physiol. Rev.* **84**, 41–68
- Ekberg, J., Craik, D. J., and Adams, D. J. (2008) Conotoxin modulation of voltage-gated sodium channels. *Int. J. Biochem. Cell Biol.* **40**, 2363–2368
- Lewis, R. J., Dutertre, S., Vetter, I., and Christie, M. J. (2012) *Conus* venom peptide pharmacology. *Pharmacol. Rev.* **64**, 259–298
- Zhang, M. M., Gruszczynski, P., Walewska, A., Bulaj, G., Olivera, B. M., and Yoshikami, D. (2010) Cooccupancy of the outer vestibule of voltage-gated sodium channels by micro-conotoxin KIIIA and saxitoxin or tetrodotoxin. *J. Neurophysiol.* **104**, 88–97
- Stephan, M. M., Potts, J. F., and Agnew, W. S. (1994) The micro1 skeletal

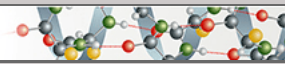
- muscle sodium channel: mutation E403Q eliminates sensitivity to tetrodotoxin but not to μ -conotoxins GIIIA and GIIIB. *J. Membr. Biol.* **137**, 1–8
14. Dudley, S. C., Jr., Todt, H., Lipkind, G., and Fozzard, H. A. (1995) A μ -conotoxin-insensitive Na^+ channel mutant: possible localization of a binding site at the outer vestibule. *Biophys. J.* **69**, 1657–1665
 15. Leipold, E., Markgraf, R., Miloslavina, A., Kijas, M., Schirmeyer, J., Imhof, D., and Heinemann, S. H. (2011) Molecular determinants for the subtype specificity of μ -conotoxin SIIIA targeting neuronal voltage-gated sodium channels. *Neuropharmacology* **61**, 105–111
 16. Choudhary, G., Aliste, M. P., Tieleman, D. P., French, R. J., and Dudley, S. C., Jr. (2007) Docking of μ -conotoxin GIIIA in the sodium channel outer vestibule. *Channels* **1**, 344–352
 17. Stevens, M., Peigneur, S., and Tytgat, J. (2011) Neurotoxins and their binding areas on voltage-gated sodium channels. *Front. Pharmacol.* **2**, 71
 18. Olivera, B. M., Rivier, J., Clark, C., Ramilo, C. A., Corpuz, G. P., Abogadie, F. C., Mena, E. E., Woodward, S. R., Hillyard, D. R., and Cruz, L. J. (1990) Diversity of *Conus* neuropeptides. *Science* **249**, 257–263
 19. Trivedi, M. V., Laurence, J. S., and Siahaan, T. J. (2009) The role of thiols and disulfides on protein stability. *Curr. Protein Pept. Sci.* **10**, 614–625
 20. Bulaj, G., West, P. J., Garrett, J. E., Watkins, M., Marsh, M., Zhang, M. M., Norton, R. S., Smith, B. J., Yoshikami, D., and Olivera, B. M. (2005) Novel conotoxins from *Conus striatus* and *Conus kinoshitai* selectively block TTX-resistant sodium channels. *Biochemistry* **44**, 7259–7265
 21. Holford, M., Zhang, M. M., Gowd, K. H., Azam, L., Green, B. R., Watkins, M., Ownby, J. P., Yoshikami, D., Bulaj, G., and Olivera, B. M. (2009) Pruning nature: biodiversity-derived discovery of novel sodium channel blocking conotoxins from *Conus bullatus*. *Toxicon* **53**, 90–98
 22. Van Der Haegen, A., Peigneur, S., and Tytgat, J. (2011) Importance of position 8 in μ -conotoxin KIIIA for voltage-gated sodium channel selectivity. *FEBS J.* **278**, 3408–3418
 23. Fuller, E., Green, B. R., Catlin, P., Buczek, O., Nielsen, J. S., Olivera, B. M., and Bulaj, G. (2005) Oxidative folding of conotoxins sharing an identical disulfide bridging framework. *FEBS J.* **272**, 1727–1738
 24. French, R. J., Yoshikami, D., Sheets, M. F., and Olivera, B. M. (2010) The tetrodotoxin receptor of voltage-gated sodium channels—perspectives from interactions with μ -conotoxins. *Mar Drugs* **8**, 2153–2161
 25. Keller, R. (2004) *Optimizing the Process of Nuclear Magnetic Resonance Spectrum Analysis and Computer Aided Resonance Assignment*. Ph.D. thesis, Swiss Federal Institute of Technology, Zürich
 26. Hwang, T. L., and Shaka, A. J. (1995) Water suppression that works. Excitation sculpting using arbitrary wave-forms and pulsed-field gradients. *J. Magn. Reson. A* **112**, 275–279
 27. Shaka, A. J., Lee, C. J., and Pines, J. (1988) Iterative schemes for bilinear operators; application to spin decoupling. *J. Magn. Reson.* **77**, 274–293
 28. Derome, A. E., and Williamson, M. P. (1990) Rapid-pulsing artifacts in double-quantum-filtered COSY. *J. Magn. Reson.* **88**, 177–185
 29. Piotto, M., Saudek, V., and Sklenár, V. (1992) Gradient-tailored excitation for single-quantum NMR spectroscopy of aqueous solutions. *J. Biomol. NMR* **2**, 661–665
 30. Sklenar, V., Piotto, M., Leppik, R., and Saudek, V. (1993) Gradient-tailored water suppression for ^1H - ^{15}N HSQC experiments optimized to retain full sensitivity. *J. Magn. Reson. A* **102**, 241–245
 31. Schwieters, C. D., Kuszewski, J. J., Tjandra, N., and Clore, G. M. (2003) The Xplor-NIH NMR molecular structure determination package. *J. Magn. Reson.* **160**, 65–73
 32. Stein, E. G., Rice, L. M., and Brünger, A. T. (1997) Torsion-angle molecular dynamics as a new efficient tool for NMR structure calculation. *J. Magn. Reson.* **124**, 154–164
 33. Linge, J. P., Williams, M. A., Spronk, C. A., Bonvin, A. M., and Nilges, M. (2003) Refinement of protein structures in explicit solvent. *Proteins* **50**, 496–506
 34. Han, T. S., Zhang, M. M., Walewska, A., Gruszczynski, P., Robertson, C. R., Cheatham, T. E., 3rd, Yoshikami, D., Olivera, B. M., and Bulaj, G. (2009) Structurally minimized μ -conotoxin analogues as sodium channel blockers: implications for designing conopeptide-based therapeutics. *ChemMedChem* **4**, 406–414
 35. Zhang, M. M., Green, B. R., Catlin, P., Fiedler, B., Azam, L., Chadwick, A., Terlau, H., McArthur, J. R., French, R. J., Gulyas, J., Rivier, J. E., Smith, B. J., Norton, R. S., Olivera, B. M., Yoshikami, D., and Bulaj, G. (2007) Structure/function characterization of μ -conotoxin KIIIA, an analgesic, nearly irreversible blocker of mammalian neuronal sodium channels. *J. Biol. Chem.* **282**, 30699–30706
 36. Khoo, K. K., Feng, Z. P., Smith, B. J., Zhang, M. M., Yoshikami, D., Olivera, B. M., Bulaj, G., and Norton, R. S. (2009) Structure of the analgesic μ -conotoxin KIIIA and effects on the structure and function of disulfide deletion. *Biochemistry* **48**, 1210–1219
 37. Schroeder, C. I., Ekberg, J., Nielsen, K. J., Adams, D., Loughnan, M. L., Thomas, L., Adams, D. J., Alewood, P. F., and Lewis, R. J. (2008) Neurologically μ -conotoxins from *Conus striatus* utilize an α -helical motif to target mammalian sodium channels. *J. Biol. Chem.* **283**, 21621–21628
 38. McArthur, J. R., Singh, G., McMaster, D., Winkfein, R., Tieleman, D. P., and French, R. J. (2011) Interactions of key charged residues contributing to selective block of neuronal sodium channels by μ -conotoxin KIIIA. *Mol. Pharmacol.* **80**, 573–584
 39. McArthur, J. R., Singh, G., O'Mara, M. L., McMaster, D., Ostroumov, V., Tieleman, D. P., and French, R. J. (2011) Orientation of μ -conotoxin PIIIA in a sodium channel vestibule, based on voltage dependence of its binding. *Mol. Pharmacol.* **80**, 219–227
 40. Hui, K., Lipkind, G., Fozzard, H. A., and French, R. J. (2002) Electrostatic and steric contributions to block of the skeletal muscle sodium channel by μ -conotoxin. *J. Gen. Physiol.* **119**, 45–54
 41. McArthur, J. R., Ostroumov, V., Al-Sabi, A., McMaster, D., and French, R. J. (2011) Multiple, distributed interactions of μ -conotoxin PIIIA associated with broad targeting among voltage-gated sodium channels. *Biochemistry* **50**, 116–124
 42. Chang, N. S., French, R. J., Lipkind, G. M., Fozzard, H. A., and Dudley, S., Jr. (1998) Predominant interactions between μ -conotoxin Arg-13 and the skeletal muscle Na^+ channel localized by mutant cycle analysis. *Biochemistry* **37**, 4407–4419
 43. Li, R. A., Ennis, I. L., French, R. J., Dudley, S. C., Jr., Tomaselli, G. F., and Marbán, E. (2001) Clockwise domain arrangement of the sodium channel revealed by μ -conotoxin (GIIIA) docking orientation. *J. Biol. Chem.* **276**, 11072–11077
 44. Tietze, A. A., Tietze, D., Ohlenschläger, O., Leipold, E., Ullrich, F., Kühn, T., Mischo, A., Buntkowsky, G., Görlach, M., Heinemann, S. H., and Imhof, D. (2012) Structurally diverse μ -conotoxin PIIIA isomers block sodium channel $\text{Na}_v1.4$. *Angew. Chem. Int. Ed. Engl.* **51**, 4058–4061
 45. Chen, R., and Chung, S. H. (2012) Binding modes of μ -conotoxin to the bacterial sodium channel (NaVAb). *Biophys. J.* **102**, 483–488
 46. Khoo, K. K., Wilson, M. J., Smith, B. J., Zhang, M. M., Gulyas, J., Yoshikami, D., Rivier, J. E., Bulaj, G., and Norton, R. S. (2011) Lactam-stabilized helical analogues of the analgesic μ -conotoxin KIIIA. *J. Med. Chem.* **54**, 7558–7566
 47. Clark, R. J., Akcan, M., Kaas, Q., Daly, N. L., and Craik, D. J. (2012) Cyclization of conotoxins to improve their biopharmaceutical properties. *Toxicon* **59**, 446–455
 48. Zuliani, V., Fantini, M., and Rivara, M. (2012) Sodium channel blockers as therapeutic target for treating epilepsy: recent updates. *Curr. Top. Med. Chem.* **12**, 962–970
 49. Shon, K. J., Olivera, B. M., Watkins, M., Jacobsen, R. B., Gray, W. R., Floresca, C. Z., Cruz, L. J., Hillyard, D. R., Brink, A., Terlau, H., and Yoshikami, D. (1998) μ -Conotoxin PIIIA, a new peptide for discriminating among tetrodotoxin-sensitive Na channel subtypes. *J. Neurosci.* **18**, 4473–4481
 50. Cruz, L. J., Gray, W. R., Olivera, B. M., Zeikus, R. D., Kerr, L., Yoshikami, D., and Moczydlowski, E. (1985) *Conus geographus* toxins that discriminate between neuronal and muscle sodium channels. *J. Biol. Chem.* **260**, 9280–9288
 51. Lewis, R. J., Schroeder, C. I., Ekberg, J., Nielsen, K. J., Loughnan, M., Thomas, L., Adams, D. A., Drinkwater, R., Adams, D. J., and Alewood, P. F. (2007) Isolation and structure-activity of μ -conotoxin TIIIA, a potent inhibitor of tetrodotoxin-sensitive voltage-gated sodium channels. *Mol. Pharmacol.* **71**, 676–685
 52. West, P. J., Bulaj, G., Garrett, J. E., Olivera, B. M., and Yoshikami, D. (2002) μ -Conotoxin SmIIIA, a potent inhibitor of tetrodotoxin-resistant sodium

Miniaturized μ -Conotoxins as Selective Na_v Blockers

- channels in amphibian sympathetic and sensory neurons. *Biochemistry* **41**, 15388–15393
53. Zhang, M. M., Fiedler, B., Green, B. R., Catlin, P., Watkins, M., Garrett, J. E., Smith, B. J., Yoshikami, D., Olivera, B. M., and Bulaj, G. (2006) Structural and functional diversities among μ -conotoxins targeting TTX-resistant sodium channels. *Biochemistry* **45**, 3723–3732
54. Favreau, P., Benoit, E., Hocking, H. G., Carlier, L., D'Hoedt, D., Leipold, E., Markgraf, R., Schlumberger, S., Córdova, M. A., Gaertner, H., Paolini-Bertrand, M., Hartley, O., Tytgat, J., Heinemann, S. H., Bertrand, D., Boelens, R., Stöcklin, R., and Molgó, J. (2012) Pharmacological characterization of a novel μ -conopeptide, CnIIIIC, indicates potent and preferential inhibition of sodium channel subtypes ($\text{Na}_v1.2/1.4$) and reveals unusual activity on neuronal nicotinic acetylcholine receptors. *Br. J. Pharmacol.* **166**, 1654–1668
55. Walewska, A., Skalicky, J. J., Davis, D. R., Zhang, M. M., Lopez-Vera, E., Watkins, M., Han, T. S., Yoshikami, D., Olivera, B. M., and Bulaj, G. (2008) NMR-based mapping of disulfide bridges in cysteine-rich peptides: application to the μ -conotoxin SxIIIa. *J. Am. Chem. Soc.* **130**, 14280–14286

**Protein Structure and Folding:
Design of Bioactive Peptides from Naturally
Occurring μ -Conotoxin Structures**

PROTEIN STRUCTURE
AND FOLDING



Marijke Stevens, Steve Peigneur, Natalia
Dyubankova, Eveline Lescrinier, Piet
Herdewijn and Jan Tytgat

J. Biol. Chem. 2012, 287:31382-31392.

doi: 10.1074/jbc.M112.375733 originally published online July 6, 2012

Access the most updated version of this article at doi: [10.1074/jbc.M112.375733](https://doi.org/10.1074/jbc.M112.375733)

Find articles, minireviews, Reflections and Classics on similar topics on the [JBC Affinity Sites](https://www.jbc.org/).

Alerts:

- [When this article is cited](#)
- [When a correction for this article is posted](#)

[Click here](#) to choose from all of JBC's e-mail alerts

Supplemental material:

<http://www.jbc.org/content/suppl/2012/07/06/M112.375733.DC1.html>

This article cites 54 references, 14 of which can be accessed free at
<http://www.jbc.org/content/287/37/31382.full.html#ref-list-1>